

**Self-consistent nonstationary processes in phase-mixed electron beams focused by mobile ions**Yu. P. Bliokh,<sup>1</sup> G. S. Nusinovich,<sup>2</sup> J. Felsteiner,<sup>1</sup> and V. L. Granatstein<sup>2</sup><sup>1</sup>*Department of Physics, Technion, 32000 Haifa, Israel*<sup>2</sup>*IREAP, University of Maryland, College Park, Maryland 20742-3511*

(Received 21 May 2002; published 20 November 2002)

This paper is devoted to the analysis of nonstationary self-consistent processes in electron beam propagation in the presence of mobile ions. This problem is of particular interest for the recently developed plasma-assisted slow-wave oscillators (pasotrons). In pasotrons beam focusing is provided by ions (in contrast to other high-power microwave sources where the beam is focused by a strong external magnetic field). Typically, pasotrons operate in rather long pulses with a pulse duration on the order of 100  $\mu$ s and larger. In such a time scale, the ion motion can play a significant role, and therefore, the self-consistent nonstationary processes in the beam transport and ion motion become important. In particular, the interaction with beam electrons may result in ion axial acceleration. In the present paper, a theory that describes these nonstationary self-consistent processes is developed, taking account of the phase mixing of electrons having a spread in their initial transverse velocities. The paper also contains some simulation results obtained for typical pasotron parameters.

DOI: 10.1103/PhysRevE.66.056503

PACS number(s): 41.85.Ja, 84.40.Fe, 52.59.Px

**I. INTRODUCTION**

The interest in the ion focusing of electron beams has a long history. This effect by itself is present practically everywhere, where electron beams propagate, because they never propagate in absolute vacuum. In any beam transport channel, there is a residual gas, which, once the beam is injected, gets ionized due to the beam impact ionization. (Of course, the ions can also be produced from neutral gas by using some laser preionization techniques as well as by other means). Then, the beam space charge quickly ejects plasma electrons leaving an ion core. The presence of ions neutralizes the beam space charge, and thus weakens the beam divergence caused by the radial electric self-field. When the gas-plasma density is high enough, the beam divergence can be suppressed completely, and therefore, due to this ion focusing, the beam can be transported via a long distance. Such an ion focusing is known as the Bennett pinch [1].

The beam divergence caused by the radial electric self-field, as known (see, e.g., Refs. [2–4]), is also compensated, to some extent, by the Lorentz force caused by the azimuthal magnetic self-field. The latter force is  $\beta^2$  times smaller than the former one (here  $\beta$  is the electron axial velocity  $v_z$  normalized to the speed of light). Therefore, this Lorentz force starts playing an important role when the beam voltage is high enough. As follows from the known beam envelope equation [2–4], to focus a beam the following condition should be fulfilled:  $f > 1/\gamma^2$ . Here  $f = n_i/n_b$  is the ion to electron beam density ratio and  $\gamma = (1 - \beta^2)^{-1/2}$  is the Lorentz factor of electrons. This condition is known as the Budker condition for beam focusing [5]. As follows from it, to focus relativistic electron beams, it is enough to have a relatively low ion density.

This fact, as well as the possibility to avoid the use of focusing magnets and solenoids, attracted a great attention to the ion focusing of high-current relativistic electron beams during the 1970s and 1980s (see, e.g., Refs. [6–9] and references therein). Since the pulse duration of these beams was typically rather short (tens to hundreds of nanoseconds), the treatment of this problem was practically always done under

the assumption that ions are immobile. As an exclusion from this rule, it is worth mentioning Refs. [10,11], where an experimental study of some effects caused by the ion motion (ion hose instability) in microsecond long pulse electron beams is described.

During the 1990s, a new plasma-filled source of coherent microwave radiation was proposed and actively studied, named the pasotron (plasma-assisted slow-wave oscillator) [12–14]. One of the specific features of the pasotron is the fact that in this device the transport of a high-perveance electron beam is provided by the Bennett pinch. A number of theoretical issues related to the beam-wave interaction in the pasotron have been recently analyzed in Refs. [15–17]. Also, some nonstationary phenomena in the beam transport in the process of gas ionization in pasotrons were recently considered in Ref. [18]. In Ref. [18], however, the effect of phase mixing of electron trajectories was neglected, while, under certain conditions, it can be important for the beam propagation.

The most important feature, which makes the beam transport in pasotrons different from the transport of relativistic electron beams studied earlier, is the length of the beam pulse duration, which in pasotrons is much longer (up to hundreds of microseconds) than in relativistic beams. In this time scale the ion motion, in accordance with the estimates made elsewhere [14,18], can play a role. For example, in the case of an axially nonuniform gas density profile, the axial motion of ions increases the ion density in regions of low gas density, and thus, improves the beam focusing there [18].

Note that the effects of ions on the operation of vacuum microwave tubes have been studied in many papers. One of the first seminal papers was Ref. [19], in which some modulations in the electron beam current were explained by the presence of ions capable of a quasiperiodic release from the potential well formed by the beam space charge (so-called ion relaxation oscillations). In spite of a long history of this problem, the effect of ions on the operation of vacuum tubes is still actively studied even nowadays (see, e.g., Refs. [20,21], and references therein). These studies, however, deal with the beams guided by external magnetic fields providing

a one-dimensional (1D) electron beam motion. When these fields are periodic (like in the case of periodic permanent magnets), this periodicity may cause a beam scalloping, which can be the reason for ion trapping. Note that in all these devices the presence of ions is inessential for electron motion. On the contrary, we are concerned about the ion focused beam propagation in the absence of guiding external fields. In such a case, first, all particles may exhibit a 3D motion, and second, the only fields which are present in a system are the self-fields of the electron beam and ions, which makes the problem under study self-consistent. An interest in this problem was motivated by some experiments with pasotrons [13,14], in which strong pulsations in the collector current have been observed. These oscillations can stem from possible pulsations of the ion density, which, being accelerated by an axially inhomogeneous electron beam, may acquire enough energy for penetrating through the potential well. Such ion pulsations may also cause pulsations in the beam current, thus making the process self-consistent.

In the present paper we make an attempt to develop a theory describing these self-consistent nonstationary processes. The paper is organized as follows. In Sec. II a simple model describing the physical effects under study is considered. In Sec. III equations are derived, which are later used for more accurate analytical and numerical studies. In Sec. IV we present some results of the analytical theory and numerical simulations. In Sec. V we interpret the results obtained in terms of pasotron parameters and present some simulation results for parameters typical for pasotron experiments. Finally, Sec. VI summarizes our considerations. In addition to the main part of the paper, there is an appendix in which electron oscillations in an anharmonic potential well are analyzed.

## II. SIMPLE MODEL OF SELF-CONSISTENT PROCESSES IN A PHASE-MIXED, ION-FOCUSED ELECTRON BEAM

When an initially quasilaminar electron beam enters an ion filled region, it experiences ion focusing. The waist of the beam in the first focal plane depends on the beam emittance. After passing this plane, electrons exhibit betatron oscillations in the anharmonic potential well formed by the focusing force of the ion channel and the defocusing force caused by the finite emittance. In such a well, the electrons with different initial transverse velocities oscillate with different frequencies, which causes the beam phase mixing. The phase-mixed beam reaches its stationary state at a distance of about several betatron wavelengths. Below we shall assume that our system is long enough, and hence, such a stationary state can be reached. In turn, the radial profile of the phase-mixed beam density determines the potential well in which the ions can move. So, after a certain time, the radial profile of the ion density will also be redistributed and, as a result, a stationary self-consistent radial distribution of both the ion and beam electron densities in the phase-mixed beam will be reached. A typical time of this transition process is the time of ion transverse oscillations, which for pasotrons is on the order of 1  $\mu$ s or less [18].

Let us consider the stability of the phase-mixed electron beam with respect to the local perturbation in the ion density. In the absence of perturbations, in an axially uniform system, the potential  $\varphi$  obeys the 1D Poisson equation

$$\frac{1}{r} \frac{\partial}{\partial r} \left( r \frac{\partial \varphi}{\partial r} \right) = 4\pi e(n_i - n_b), \quad (1)$$

with the following boundary condition at the wall of a radius  $R_w$ :  $\varphi(R_w) = 0$ . The potential at  $r=0$  which we will use below for crude estimates, as follows from Eq. (1), is equal to

$$\varphi = \varphi(0) = - \left( \frac{I_b}{v_x} - eN_i \right) \left( 1 + 2 \ln \frac{R_w}{a} \right), \quad (2)$$

where  $a$  is the beam radius and  $N_i$  is the ion density per unit length. It is assumed above that the beam and the ion channel radii are equal and that the beam and ion densities are homogeneous. When the beam or wall radii and/or the ion density slowly depend on  $z$ , so also the potential does. This dependence means that an axial electric field,  $E_z = -\partial\varphi/\partial z$ , appears in the system, which causes the ion axial motion. The action of this field on the beam electrons can be neglected since the beam electron energy greatly exceeds  $e\varphi$ .

Now let us consider the effect of the local ion perturbation on this equilibrium state. Let us assume that the longitudinal scale of this perturbation is larger than the beam radius  $a$ , but smaller than the betatron wavelength  $\lambda_b = 2\pi a(I_A/I_b)^{1/2}$ . Here  $I_A = (mc^3/e)\beta\gamma$  is the Alfvén current. This assumption allows us to use Eq. (1) and its solution given by Eq. (2) for analyzing the effect of ion perturbations on the potential. An additional number of ions causes beam compression. This means that after a beam passes the region of ion perturbation with  $\delta N_i > 0$ , the beam envelope radius decreases:  $da/dz < 0$ .

The ion density  $N_i$  and velocity  $v_i$  obey, respectively, the continuity equation

$$\frac{\partial N_i}{\partial t} + \frac{\partial}{\partial z} (N_i v_i) = 0 \quad (3)$$

and the equation for ion motion

$$\frac{\partial v_i}{\partial t} + v_i \frac{\partial v_i}{\partial z} = - \frac{e}{m_i} \frac{\partial \varphi}{\partial z}. \quad (4)$$

In the equilibrium state, the ion density per unit length and the beam radius are constant and the ion axial velocity equals zero. Thus, the perturbations of the ion density and the ion velocity obey linearized equations (3) and (4):

$$\frac{\partial \delta N_i}{\partial t} + N_{i0} \frac{\partial v_i}{\partial z} = 0, \quad (5)$$

$$\frac{\partial v_i}{\partial t} = - \frac{e}{m_i} \left( \frac{\partial \varphi}{\partial N_i} \Big|_{N_{i0}} \frac{\partial \delta N_i}{\partial z} + \frac{\partial \varphi}{\partial a} \Big|_{a_*} \frac{\partial \delta a}{\partial z} \right). \quad (6)$$

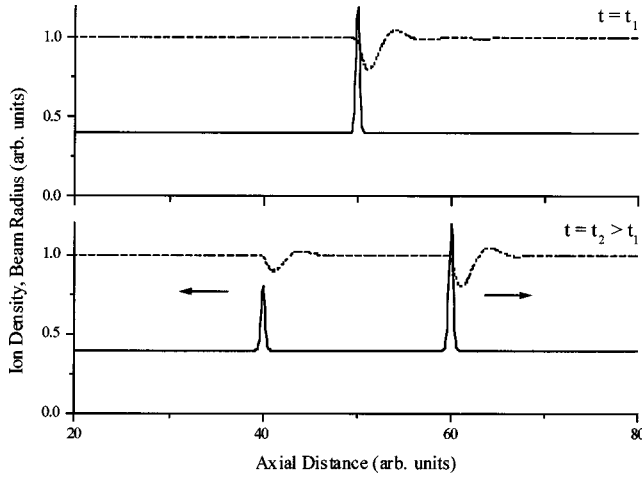


FIG. 1. Ion density (solid line) and beam current radius (dashed line) for two instants of time.

Here  $\delta a$  is the perturbation in the beam envelope radius due to the ion density perturbation  $\delta N_i$ . Two derivatives of the potential in the right-hand side (RHS) of Eq. (6) are positive and equal to

$$\left. \frac{\partial \varphi}{\partial N_i} \right|_{N_{i0}} = e \left( 1 + 2 \ln \frac{R_w}{a_*} \right) > 0, \quad (7)$$

$$\left. \frac{\partial \varphi}{\partial a} \right|_{a_*} = 2 \left( \frac{I_b}{v_z} - e N_{0i} \right) a_*^{-1} > 0. \quad (8)$$

If we neglect the last term in the RHS of Eq. (6), Eqs. (5) and (6) yield the wave equation

$$\frac{\partial^2(\delta N_i)}{\partial t^2} - \frac{e^2 N_{0i}}{m_i} \left( 1 + 2 \ln \frac{R_w}{a_*} \right) \frac{\partial^2(\delta N_i)}{\partial z^2} = 0, \quad (9)$$

which describes the propagation of ion density waves in  $\pm z$  directions with the phase velocity

$$v_{\text{ph}} = \sqrt{\frac{e^2 N_{0i}}{m_i} \left( 1 + 2 \ln \frac{R_w}{a_*} \right)}. \quad (10)$$

The presence of the last term in the RHS of Eq. (6) results in a different effect. Since an addition of ions focuses the beam stronger, in the region of ion fluctuation  $\partial(\delta a)/\partial z < 0$ . So, this second term represents a positive force. Accounting for this term in the ion wave propagation described above causes the deceleration of the ion wave propagating backward and the acceleration of the wave propagating forward. Since the velocity and density perturbations are proportional to each other, the deceleration of the backward wave results in its attenuation, while the acceleration of the forward wave results in its amplification, as shown in Fig. 1.

Let us emphasize the role of the phase mixing of electron betatron oscillations in this process. Once we assume that the beam electrons exhibit betatron oscillations, whose period does not depend on the amplitude of oscillations of individual electrons, it follows that perturbations in the beam radius and, therefore, in the potential  $\varphi$ , caused by the first

ion fluctuation (backward ion wave), will continue to oscillate behind it in the direction of the beam propagation. Correspondingly, the second ion fluctuation (forward ion wave) can experience the effect of the variation of the potential  $\varphi$ , caused by the ion wave propagating backward. However, the electrons oscillate in an anharmonic potential well. Therefore, these betatron oscillations decay at a distance of the order of a few betatron periods. As a result, after the propagation of ion fluctuations, which move in the opposite direction over a distance larger than several betatron periods, these fluctuations propagate and evolve independently of each other.

### III. GENERAL FORMALISM

In this section we shall derive equations for the ion-focused beam envelope in the phase-mixed stage and equations describing the ion motion.

In Sec. II we considered a stationary beam of transversely oscillating electrons whose oscillation phases in the phase-mixed state are uniformly distributed from 0 to  $2\pi$ . Strictly speaking, such a beam needs a kinetic description. For our purpose, however, it is enough to mention that this stationary beam is formed as a result of the electron motion in the self-consistent potential, and therefore, is characterized by a large spread in the transversal oscillations energy. This spread is of the order of the difference of the potentials on the axis and at the beam envelope radius. Correspondingly, the spread in amplitudes of electron oscillations is of the order of the beam envelope radius. The angular momentum  $M = m \gamma r v_0$  of each particle is an integral of motion, therefore its value is determined by the boundary conditions at the entrance. The motion of such a particle with a given angular momentum is the motion in the 1D potential field. In general, such a particle should exhibit oscillations whose period depends on the particle total energy, because it oscillates in the anharmonic potential well. These two features, a large spread in the amplitudes of electron oscillations and the nonisochronism of the transverse betatron oscillations, are extremely important because they cause the phase mixing of electron oscillations and damping of the beam envelope oscillations [9,22].

After the phase mixing of betatron oscillations, the beam reaches its stationary state. In general, the beam envelope equation for a phase-mixed electron beam can be written as [see Eq. (4.49) in Ref. [4]]

$$\frac{d^2 a}{dz^2} = \frac{2I_b}{I_A \beta^2} (\gamma^2 - f) \frac{1}{a} + \frac{\langle M^2 \rangle}{m^2 \gamma^2 v_z^2} \frac{1}{a^3}, \quad (11)$$

where  $f = N_i e v_z / I_b$  is the ratio of the ion to electron beam densities per unit length and  $\langle M^2 \rangle$  is the mean value of the squared angular momentum, which is proportional to the beam emittance. So, when  $f > 1/\gamma^2$  (Budker condition), the first term on the RHS in Eq. (11) describes the beam compressing force, while the second one describes the beam expansion force caused by the finite transverse ‘‘temperature’’ of the beam. The beam equilibrium occurs when these two forces compensate for each other. A corresponding equilibrium radius  $a_*$ , as follows from Eq. (11), is equal to

$$a_* = \sqrt{\frac{\langle M^2 \rangle I_A}{2I_b(f - \gamma^{-2})m^2 \gamma^2 c^2}}. \quad (12)$$

Note that, strictly speaking, the radius  $a$  has the meaning of a scale-beam radius (see, e.g., Ref. [22]).

Coming back to Eq. (11), we should emphasize one fact which is very important for the applicability of this equation. Usually, this equation is used just for defining the beam envelope radius in the equilibrium state. However, according to this equation, the beam envelope radius, at least when the space charge compensation factor  $f$  is constant, can exhibit axial oscillations with a constant amplitude. At the same time, as was mentioned above, numerical simulations clearly indicate [22] that the electron anharmonic betatron oscillations cause a damping of these beam envelope oscillations. This means that to be able to describe this damping, Eq. (11) should be properly modified. Since the damping originates from the anharmonicity of the betatron oscillations of individual electrons, we should start from considering this anharmonicity in more detail. Such a consideration is carried out in the Appendix. As is shown there, the spatial frequency of anharmonic betatron oscillations of individual electrons is equal to

$$k = k_\beta \left[ 1 + \frac{15}{16} \sqrt{\frac{M^2}{\langle M^2 \rangle}} \left( 1 - \frac{M^2}{\langle M^2 \rangle} \right) \frac{b^2}{a_*^2} \right]. \quad (13)$$

Here  $b$  is the amplitude of oscillations of an individual particle and  $k_\beta$  is the spatial frequency of the small amplitude betatron oscillations,

$$k_\beta = 2 \sqrt{\frac{2I_b(f - \gamma^{-2})}{I_A \beta^2}} \frac{1}{a_*}. \quad (14)$$

When the angular momentum of beam electrons originates from some fluctuations causing the spread in electron perpendicular velocities, the ratio  $M^2/\langle M^2 \rangle$  in Eq. (13) is on the order of 1. Also, the amplitude of electron oscillations  $b$  can vary from zero to  $a_*$ . Therefore, the anharmonicity of these oscillations, which can be characterized by the parameter  $dk/d(b^2)$  is rather strong (on the order of  $k_\beta/a_*^2$ ), and, correspondingly, the spectrum of  $k$  determined by Eq. (13),  $\Delta k$ , is on the order of  $k_\beta$ . This means that any disturbance in the beam envelope shape will be damped due to the phase mixing at the distance on the order of one period of betatron oscillations  $2\pi/k_\beta$ .

This conclusion is confirmed by numerical simulations done for the electron motion in the presence of the self-fields and the field produced by immobile ions having a perturbation localized in  $z$ , as was described above in Sec. II. Some results of these simulations are illustrated in Fig. 2, which shows the radial size of the solid beam area containing 25% (curve I) and 50% (curve II) of the total number of particles as the function of the normalized axial coordinate. The first oscillations on the left show the beam compression after the beam injection in a space containing the ion population. After a few betatron periods the beam radius, due to the phase mixing, reaches its equilibrium. Then, the beam, which already propagates in the equilibrium state, passes through the

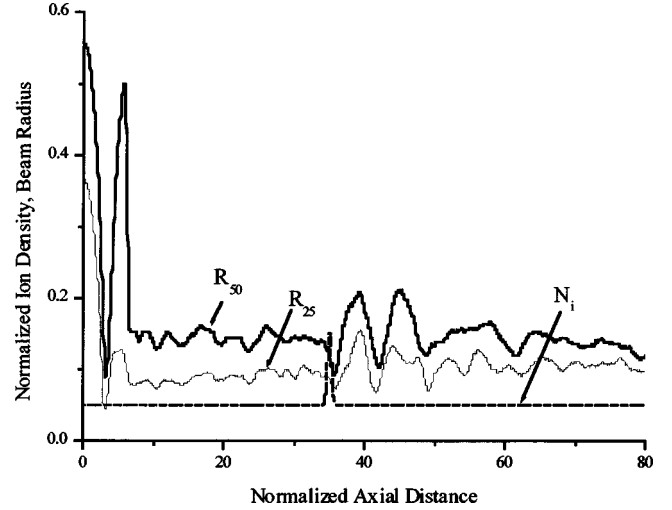


FIG. 2. Beam radius evolution from the initial to the equilibrium radius and the beam response to a local perturbation in the ion density shown by the dashed line. The thick and thin solid lines show, respectively, the beam radius, inside which 50% and 25% of the total beam current are contained.

localized ion fluctuation (ion density is shown by the dotted line). This fluctuation causes some oscillations in the beam radius. As is shown in Fig. 2, these oscillations are damped after two to three betatron periods. As shown in the Appendix, this damping is due to the anharmonicity of electron oscillations, which we just discussed above.

To qualitatively describe this damping of beam radius perturbations, one can introduce into the RHS of Eq. (11) an additional term describing the dissipation, which should be proportional to  $-A da/dz$ . Here  $A$  is a constant, which, in order to provide the damping of perturbations at the distance on the order of the betatron period, can be determined as  $A = \chi k_\beta$ , where the coefficient  $\chi$  is on the order of 1. So, the modified equation for the beam envelope can be written as [cf. Eq. (11)]

$$\frac{d^2 a}{dz^2} = \frac{2I_b}{I_A \beta^2} (\gamma^{-2} - f) \frac{1}{a} + \frac{\langle M^2 \rangle}{m^2 \gamma^2 v_z^2} \frac{1}{a^3} - \chi k_\beta \frac{da}{dz}. \quad (15)$$

Now let us discuss the equations describing the ion motion. Small perturbations in the ion density can be described in a hydrodynamic approach, which is correct in the absence of intersection of ion trajectories. When there is an intersection, which may occur either in the case of large perturbations in the density, or in an axially bounded system with particle reflection from the ends, it is necessary to model the ion motion numerically, as will be done later.

In the absence of interception and ionization process, the ion motion can be described by the continuity equation (5), which can be rewritten for the space charge neutralization factor  $f$  as

$$\frac{\partial f}{\partial t} + \frac{\partial}{\partial z} (f v_i) = 0, \quad (16)$$

and the equation for the ion motion (4), in which the potential  $\varphi$  is determined by Eq. (2).

When the process of the beam impact ionization is taken into account (this case will be considered below in Sec. IV C), Eq. (16) is replaced by the following:

$$\frac{\partial f}{\partial t} + \frac{\partial}{\partial z}(f v_i) = n_0(z) v_z \sigma, \quad (16')$$

where  $n_0(z)$  is the gas density and  $\sigma$  is the ionization cross section.

In terms of the space charge compensation factor, Eq. (2) can be rewritten as

$$\varphi = \varphi(r=0, z) = -\frac{I_b}{\nu_z} (1-f) \left( 1 + 2 \ln \frac{R_w}{a} \right). \quad (17)$$

Note that now this potential depends on the axial coordinate, because the factor  $f$  and the beam radius  $a$  are axially dependent. So, equations (15)–(17) and Eq. (4) form a self-consistent set of equations, which will be used in the following section.

## IV. RESULTS

### A. Linear theory

In the framework of the linear theory, the beam radius, the ion density (or the space charge compensation ratio  $f$ , which is proportional to it), and the ion velocity can be represented as  $a = a_* + \delta a$ ,  $f = f_0 + \delta f$ , and  $v_i = u$ , respectively. Here  $a_*$  and  $f_0$  are the stationary values of  $a$  and  $f$  and the stationary value of the ion velocity is zero. Linearizing Eqs. (4) and (15)–(17) with respect to these perturbations yields

$$\frac{d^2 \delta a}{dz^2} + \frac{1}{2} k_\beta^2 \delta a + \chi k_\beta \frac{d \delta a}{dz} = -\frac{1}{4} k_\beta^2 a_* \frac{\delta f}{f_0 - \gamma^{-2}}, \quad (18)$$

$$\frac{\partial \delta f}{\partial t} + f_0 \frac{\partial u}{\partial z} = 0, \quad (19)$$

$$\frac{\partial u}{\partial t} = -\frac{e}{m_i} \left( \frac{\partial \varphi}{\partial f} \Big|_{f_0, a_*} \frac{\partial \delta f}{\partial z} + \frac{\partial \varphi}{\partial a} \Big|_{f_0, a_*} \frac{\partial \delta a}{\partial z} \right). \quad (20)$$

Here Eqs. (19) and (20) are essentially the same Eqs. (5) and (6) which were analyzed in Sec. II, while Eq. (18) determines the relation between the beam envelope and ion density perturbations that makes this set of equations self-consistent.

Assuming that these perturbations are proportional to  $\exp[i(\kappa z - \omega t)]$ , one can easily derive from Eqs. (18)–(20) the following dispersion equation:

$$\omega^2 = \kappa^2 \frac{e \varphi_f f_0}{m_i} + \kappa^2 \frac{e \varphi_a a_* k_\beta^2}{4 m_i (f_0 - \gamma^{-2})} \times \frac{(\kappa^2 - \frac{1}{2} k_\beta^2) + i \chi k_\beta \kappa}{[(\kappa^2 - \frac{1}{2} k_\beta^2)^2 + (\chi k_\beta \kappa)^2]}. \quad (21)$$

Here we introduced the following notations:  $\varphi_a \equiv \partial \varphi / \partial a|_{f_0, a_*}$ ,  $\varphi_f \equiv \partial \varphi / \partial f|_{f_0, a_*}$ .

Let us now make some comments regarding the validity of our approach. Equation (21) is valid for the same range of wave numbers  $\kappa$  as the beam envelope equation (15). When the axial scale of ion density perturbation,  $L_i$ , is larger than the betatron wavelength  $\lambda_b$ , the ‘‘dissipative’’ term in the latter equation does not make any sense because, when  $L_i > \lambda_b$ , the beam electron oscillations can be treated as adiabatic, and hence, the phase mixing does not occur. In such a long-wavelength limit of ion perturbations, the beam envelope radius is equal to its equilibrium value  $a_*$  given by Eq. (12), which parametrically depends on  $z$  because the space charge compensation ratio  $f$  is determined by the local density of ions:  $\varphi_f \equiv \partial \varphi / \partial f|_{f_0, a_*}$ . So, the wave numbers under consideration should be larger than the betatron wave number  $k_\beta$ .

For analyzing the wave increment it is convenient to rewrite Eq. (21) in normalized variables and also take into account the definition of the potential given by Eq. (17). This yields

$$\Omega^2 = K^2 \left\{ f_0 (f_0 - \gamma^{-2}) (1 + 2 \ln R_w / a_*) + \frac{1}{2} (1 - f_0) \frac{(K^2 - \frac{1}{2}) + i \chi K}{(K^2 - \frac{1}{2})^2 + \chi^2 K^2} \right\}. \quad (22)$$

Here

$$\Omega = \omega \frac{a_*}{c} \frac{I_A \beta}{2 I_b} \left( \frac{m_i}{2m} \right)^{1/2}$$

and  $K = \kappa / k_\beta$  are the normalized frequency and axial wave number, respectively.

The analysis of this dispersion equation shows that the wave increment is maximal for the wave numbers on the order of the betatron wave number and in this region the imaginary part of the frequency is on the order of its real part. Note that in Eq. (22)  $(f_0 - \gamma^{-2})$  and  $(1 - f_0)$  are of the same order because, as the numerical results presented later show, the space charge compensation ratio  $f_0$  oscillates in the range from  $\gamma^{-2}$  to 1. So, both the frequency and the increment are predominantly determined by the value of the parameter

$$\frac{a_*}{c} \frac{I_A \beta^2}{4 I_b} \left( \frac{m_i}{m} \right)^{1/2}.$$

This is a typical time of the instability growth and also a characteristic time of temporal fluctuations in the ion and beam current densities. For typical pasotron parameters, this time is about 1–2  $\mu$ s.

### B. Nonlinear theory: Unbounded system

For numerical studies of the nonstationary, nonlinear, self-consistent processes we used Eq. (15) describing the beam envelope radius. The ion motion in the field with the potential given by Eq. (17) was described by the method of mac-

roparticles. It was assumed that each macroparticle represents a number of ions distributed over a space whose size is much smaller than the betatron wavelength, which is the axial scale of our problem. This distribution provides a smooth variation of the space charge compensation ratio  $f$  in the beam envelope equation.

Numerical simulations were carried out with the use of equations written in normalized variables:

$$\begin{aligned} \rho &= \frac{a}{a(0)}, \quad \xi = \frac{z}{a(0)\gamma} \sqrt{\frac{2I_b}{I_A\beta^2}}, \\ \tau &= t \frac{1}{a(0)\gamma} \sqrt{\frac{eI_b}{m_i v_z}} \sqrt{\frac{2I_b}{I_A\beta^2}}, \quad u = v_i \sqrt{\frac{m_i v_z}{eI_b}}, \\ \psi &= \frac{\varphi v_z}{I_b} = -(1-f) \left( 1 + 2 \ln \frac{\rho_w}{\rho} \right). \end{aligned} \quad (23)$$

Here  $a(0)$  is the beam radius at the entrance and  $\rho_w = R_w/a(0)$  is the normalized radius of the wall.

In these normalized variables Eq. (17) and the equation for ion motion have the following form:

$$\frac{d^2\rho}{d\xi^2} = (1-f\gamma^2) \frac{1}{\rho} + \frac{T_b}{\rho^3} - \chi \frac{d\rho}{d\xi}, \quad (24)$$

$$\frac{d^2\xi_i}{d\tau^2} = -\frac{\partial\psi}{\partial\xi_i}. \quad (25)$$

Here  $T_b = \langle M^2 \rangle I_A \beta^2 \gamma^2 / 2m^2 \gamma^2 v_z^2(0) I_b$  and  $\xi_i$  is the axial coordinate of the  $i$ th macroparticle. The space charge neutralization ratio is determined by

$$f(\xi) = \frac{\sqrt{\pi}}{\Delta^2} \sum_{i=1}^N q \exp\left(-\frac{(\xi - \xi_i)^2}{\Delta^2}\right), \quad (26)$$

where  $q_i$  is the charge of the  $i$ th macroparticle normalized to the electron charge  $e$  and  $N$  is the total number of macroparticles. The initial condition for macroparticle location, which describes a local perturbation of the ion density, was given as  $\xi_{i+1}(0) = \xi_i(0) + h/[1 + \Delta f \exp(-[\xi_i(0) - \xi_0]^2/\Delta_0^2)]$ . Here  $h$  is the step characterizing the distance between macroparticles,  $\xi_0$  is the coordinate of a center of ion perturbation,  $\Delta f$  is its amplitude, and  $\Delta_0$  is the scale of this localization.

Let us start presenting our results from considering the dynamics of the initially localized perturbation of ion density, which we discussed above. The results of simulations are shown in Fig. 3. The ion waves shown in this figure originate from a small initial perturbation of ion density.

The dynamics of these two, copropagating and contrapropagating waves agrees well with the results of our qualitative analysis carried out in Sec. II: the backward wave decays, while the forward wave grows. An interesting peculiarity of the solution shown in Fig. 3 is the existence of oscillations in the region between two, copropagating and contrapropagating waves. These oscillations can be explained by the fact that, as follows from Eq. (23), the local perturbations in ion density cause perturbations in the beam

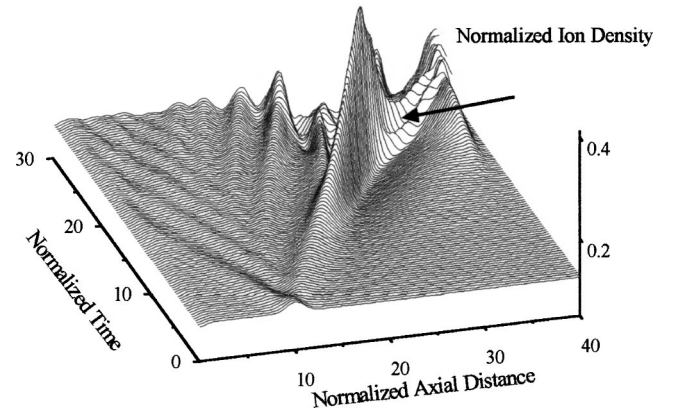


FIG. 3. Space and time evolution of a small local perturbation in the ion density in the axially unbounded system. The arrow points to the bunch of accelerated ions.

envelope after electrons pass through this localized region. Then, these perturbations in the beam envelope provoke secondary perturbations in the ion density, which in the presence of the attenuation due to the phase mixing are significant at distances on the order of the betatron wavelength and smaller.

As the amplitude of the ion wave propagating along the beam increases, the nonlinearity in the ion motion increases as well. This leads to the wave turnover and to the appearance of a bunch of accelerated ions, shown in Fig. 3 by an arrow. The velocity of ions in such a bunch is larger than the wave phase velocity. This indicates the appearance of the ion acceleration mechanism. Recall that such an ion self-acceleration at the expense of a certain deceleration of an ion-pinch electron beam was already discussed in Sec. II.

### C. Nonlinear theory: Bounded system

So far, we have considered the processes in an axially unbounded system and assumed that the ions are “prepared” before the beam injection. In real devices, however, the ions are produced from a neutral gas by the beam electrons and also the potential in the entrance and exit cross sections is equal zero. The latter leads to the formation of an axial potential well due to the beam space charge field. Far enough from these cross sections, the potential can be described by Eq. (17) [see also the normalized potential  $\psi(\xi)$  in Eq. (23)]. Recall that this potential already depends on the axial coordinate, because the ion density and the beam envelope radius are axially dependent. In order to take into account the effect of entrance and exit cross sections, it makes sense to replace  $\psi(\xi)$  by the product  $\mu(\xi)\psi(\xi)$ . The additional function  $\mu(\xi)$  can be determined as

$$\mu(\xi) = \left[ 1 - \exp\left(-q \frac{\xi}{l}\right) \right] \left[ 1 - \exp\left(-q \frac{(l-\xi)}{l}\right) \right], \quad (27)$$

where parameter  $q$  should be large enough for localizing the edge effects,  $l$  is the normalized coordinate of the exit. Certainly, the appearance of the axial potential well will lead to the reflection of ion waves from potential barriers near the

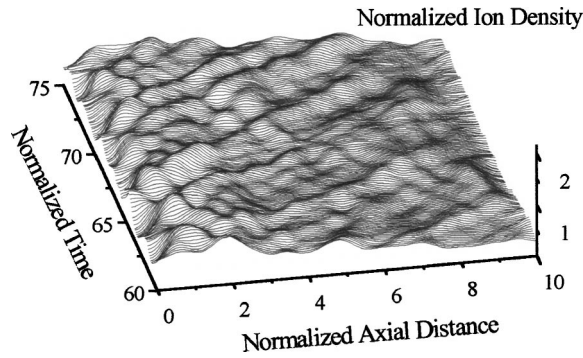


FIG. 4. Space and time evolution of a small local perturbation in the ion density in the axially bounded system.

entrance and the exit, and hence, cause the superposition and interference of these fluctuations.

To account for the process of the beam impact ionization, we considered the total number of macroparticles  $N$  as a function of time, which, due to ionization, increases in time proportionally to the RHS term in Eq. (16'). The dimensionless form of this source term is

$$S = n_0 \sigma v_z \gamma a(0) \sqrt{\frac{I_A \beta^2}{2I_b}} \sqrt{\frac{m_i v_z}{e I_b}}. \quad (28)$$

It was assumed that the gas density decays exponentially along the axis. Correspondingly, in Eq. (28) the gas density  $n_0$  was given as  $n(0)\exp(-\xi/l_g)$ . The value of  $S=1$  corresponds to the creation of such a number of ions in the time step  $\Delta\tau=1$  at the distance  $\Delta\xi=1$ , which causes a complete neutralization of the beam space charge.

An example of the spatial-temporal evolution of the ion density in the bounded system in the presence of the beam impact ionization is shown in Fig. 4. Here the local space-charge neutralization ratio  $f$  is shown as the function of the normalized time and axial coordinate. The results presented in Fig. 4 correspond to the normalized scale of the gas inhomogeneity  $l_g=4.0$ . As one can see in Fig. 4, the system exhibits the ion wave motion and the filaments shown in this figure can be attributed to the ion acceleration.

As the total number of ions trapped by the potential well increases, the potential barrier decreases, because the beam space charge gets compensated. Correspondingly, the effect of ion acceleration becomes more important. Indeed, when the ion density is high enough, the ions compensate for the beam space charge almost completely. Therefore, even a small ion acceleration allows them to penetrate through a small potential barrier. Thus, in such a state, some kind of equilibrium occurs, in which the beam impact ionization as the source of new ions and the release of accelerated ions from the potential well compensate for each other. Of course, this equilibrium is not static, and the beam radius and the ion density oscillate about their equilibrium values. An example of such oscillations is shown in Fig. 5, which shows the total number of ions in the system and the beam radius at the collector (exit) as functions of time. Note that here the total space-charge compensation ratio is shown, which is determined by the total number of ions trapped by the potential

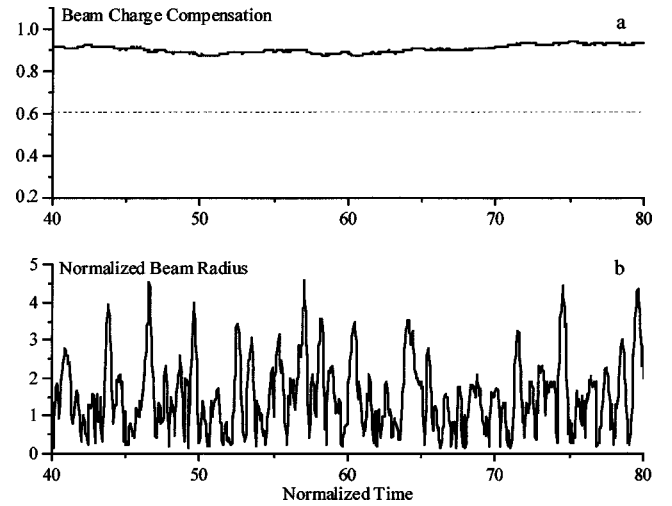


FIG. 5. Temporal evolution of the total number of trapped ions or space-charge compensation ratio (a) and the beam radius at the collector (b).

well. From comparison of this dependence with results shown in Fig. 3 and 4 it follows that even when the local oscillations of the ion density shown in these figures are large, the total number of ions exhibits only weak oscillations. At the same time even these weak oscillations may cause significant oscillations of the beam radius.

## V. DISCUSSION: APPLICATION TO THE PASOTRON

Let us estimate the values of the normalized parameters used above for the pasotron experiments carried out at Hughes Research Lab and at the University of Maryland [23]. In these experiments the device was driven by an electron beam with the typical range of voltages from 36 to 40 kV and currents from 30 to 50 A. These values of the beam voltage and current correspond to  $\beta \approx 0.375-0.38$ ,  $\gamma \approx 1.08$ , and  $I_A \approx 6.5$  kA. Correspondingly, the beam current to Alfvén current ratio is about 0.005.

The normalized time  $\tau$  can be represented as  $t/t_*$ , where the normalization time  $t_*$  is equal to  $[a(0)/c][I_A/I_b]\beta[(\gamma/2)(m_p/m)A]^{1/2}$ , where  $A$  is the atomic number of the gas and  $m_p$  is the proton mass. For the beam radius at the entrance equal to 2 cm and other parameters given above, this yields  $t_* = 0.16\sqrt{A}$   $\mu\text{sec}$ . Correspondingly, for the normalized axial coordinate determined as  $\xi = z/z_*$ , the normalization length  $z_*$  is approximately equal to 8 cm.

The betatron wave number, in accordance with Eq. (14), is inversely proportional to the equilibrium radius of the beam envelope  $a_*$ . For a typical value of this radius of about 1 cm, the betatron wave number is equal to  $0.2 \text{ cm}^{-1}$  and the period of betatron oscillations is about 30 cm. Since the equilibrium radius of the beam envelope and the average squared initial angular momentum  $\langle M^2 \rangle$  are proportional to each other as given by Eq. (12), the choice of the equilibrium radius determines the momentum  $\langle M^2 \rangle$ .

We also studied some nonstationary phenomena in the beam current density and charge compensation ratio for typi-

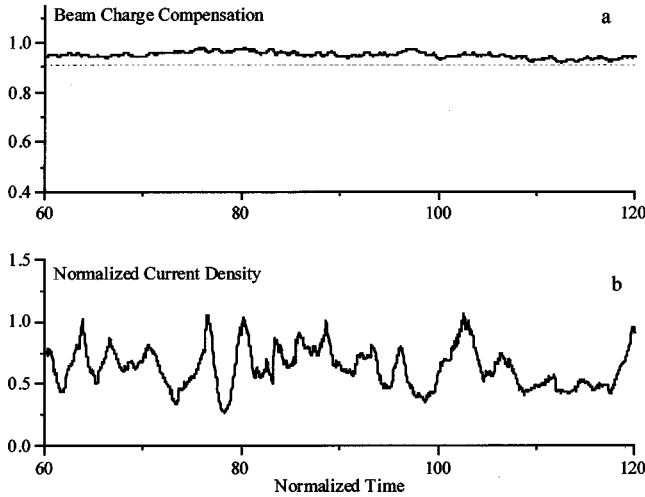


FIG. 6. Temporal evolution of the total space-charge compensation ratio (a) and the normalized beam current density (b) in the pasotron.

cal pasotron parameters. Simulations were done for the pasotron with the beam voltage and current equal to 35 kV and 30 A, respectively. It was assumed that the beam propagates in a wave guide of a radius of 3 cm and a length of 80 cm. It was also assumed that the initial beam radius at the entrance is equal to 2 cm, while the equilibrium beam radius  $a_*$  is equal to 1 cm, which corresponds to the angular spread of  $\langle \alpha^2 \rangle^{1/2} = 0.05$  and the normalized temperature  $T = 0.035$ . The He pressure at the entrance was taken equal to  $4 \times 10^{-4}$  Torr, so the corresponding ionization time at the entrance is equal to 10  $\mu\text{sec}$ . This choice of the device parameters yields a normalization time  $t_* = 0.32 \mu\text{sec}$  and a normalization length  $z_* = 8.0$  cm. These values result in the following values of the normalized parameters adopted in our theory: the source term  $S = 3.2 \times 10^{-2}$ , the normalized length  $l = 10$ , the normalized scale of the gas density profile  $l_g = 4.0$ . We also assumed that the dissipation coefficient  $\chi$  is equal to 0.5.

Results are presented in Figs. 6(a) and 6(b). Here, Fig. 6(a) shows the ratio of a total charge of all ions in the interaction space to the total number of all electrons there. The dotted straight line in Fig. 6(a) corresponds to the ion density, at which the beam focusing starts. (In other words, this is the case when the initial beam radius is equal to the equilibrium radius.) As one can see, the charge compensation ratio fluctuates in a rather small range of values close to 1. A typical scale of these temporal oscillations in the beam current density and charge compensation ratio is on the order of several units of  $t_*$  or, in other words, on the order of 1 ms. Of course, fluctuations in the ion density affect the axial velocity of electrons, which in pasotron amplifier configurations may result in additional fluctuations of the phase of the output signal. This issue, which is extremely important for the performance of amplifiers, is, however, beyond the scope of the present study.

Figure 6(b) shows the beam current density normalized to the density, which corresponds to the beam with an equilibrium radius. Strong fluctuations in the beam current density

shown here indicate that there also should be strong oscillations in the beam current density and the size of the beam area deposition at the collector. Results presented in Fig. 6(b) are quite similar to experimental observations of fluctuations in the beam current shown in Fig. 14 of Ref. [13].

## VI. SUMMARY

A theory describing the self-consistent nonstationary processes in the propagation of a phase-mixed electron beam through a nonuniform column of mobile ions is developed. It is shown that in plasma-assisted slow-wave oscillators these processes may result in substantial temporal oscillations of the beam current density. Also, these processes may cause acceleration of ions.

## ACKNOWLEDGMENTS

This work has been supported by the United States-Israel Bi-national Science Foundation and the Air Force Office of Scientific Research (New World Vistas program, Grant No. F496209710270). The authors are also indebted to D. M. Goebel for very useful discussions of issues addressed in the present study.

## APPENDIX: ELECTRON OSCILLATIONS IN AN ANHARMONIC POTENTIAL WELL

As known [24], the transverse motion of electrons, which have initial nonzero transverse velocities, in the 1D potential well,  $U_{\text{eff}}(r)$ , obeys the following equation:

$$m\gamma \frac{d^2 r}{dt^2} = -\frac{\partial U_{\text{eff}}}{\partial r}, \quad (\text{A1})$$

where the effective potential well is determined as

$$U_{\text{eff}} = e\varphi_{\text{eff}} + \frac{M^2}{2m\gamma r^2}. \quad (\text{A2})$$

In Eq. (A2)  $M = m\gamma r v_\theta$  is the angular momentum, which is the invariant of motion. The potential  $\varphi_{\text{eff}}(r)$ , in accordance with Eq. (1) and the fact that the beam electric self-field is partly compensated by the magnetic self-field, is equal to

$$\varphi_{\text{eff}}(r) = -\left[ \frac{I_b}{v_z} (1 - \beta^2) - eN_i \right] \left( 1 + 2 \ln \frac{b}{a} - \frac{r^2}{a^2} \right). \quad (\text{A3})$$

Correspondingly, Eq. (A1) can be rewritten as

$$\frac{d^2 r}{dt^2} = 2 \frac{eI_b}{mc^3} - \frac{c^2}{a^2 \beta_z \gamma^3} (1 - \gamma^2 f) r + \frac{M^2}{m^2 \gamma^2 r^3}. \quad (\text{A4})$$

The electron radius in the equilibrium state, as follows from Eq. (A4), is equal to

$$r_0^4 = \frac{M^2}{m^2 \gamma^2 c^2} \frac{I_A}{2I_b (f - \gamma^{-2})} a^2. \quad (\text{A5})$$

When the beam radius is equal to its equilibrium value given by Eq. (12),  $a = a_*$ , Eq. (A5) yields a very simple relation between  $r_0$  and  $a_*$ :

$$r_0^4 = a^4 \frac{M^2}{\langle M^2 \rangle}. \quad (\text{A6})$$

Now let us consider small oscillations of the electron radius about this equilibrium state:  $r = r_0(1+x)$ . A proper expansion of the RHS of Eq. (A4) in terms of  $x$ , which implies the account for the second- and third-order terms in the last term in this equation (cf. Ref. [24]), reduces Eq. (A4) to

$$\frac{d^2x}{dz^2} + k_\beta^2 x + \frac{k_\beta^2}{2} \frac{M^2}{\langle M^2 \rangle} (-3x^2 + 5x^3) = 0. \quad (\text{A7})$$

Here the frequency of the betatron oscillations  $k_\beta$  is determined by Eq. (14). Equation (A7) describes anharmonic oscillations, whose frequency of spatial oscillations depends on the oscillation amplitude as [23]

$$k = k_\beta + \left( \frac{3c_3}{8k_\beta} - \frac{5c_2^2}{12k_\beta^3} \right) x_1^2. \quad (\text{A8})$$

Here  $x_1$  is the amplitude of oscillations with the frequency  $k_\beta$  and  $c_2$  and  $c_3$  are coefficients at the corresponding powers of  $x$  in Eq. (A7). Substituting the values of these coefficients into Eq. (A8) results in

$$k = k_\beta \left[ 1 + x_1^2 \frac{15}{16} \frac{M^2}{\langle M^2 \rangle} \left( 1 - \frac{M^2}{\langle M^2 \rangle} \right) \right]. \quad (\text{A9})$$

The amplitude  $b$  of electron oscillations about the equilibrium state relates to  $x_1$  as  $b = r_0 x_1$ . Therefore, using Eq. (A6), one can finally rewrite Eq. (A9) as

$$k = k_\beta \left[ 1 + \frac{15}{16} \sqrt{\frac{M^2}{\langle M^2 \rangle}} \left( 1 - \frac{M^2}{\langle M^2 \rangle} \right) \frac{b^2}{a_*^2} \right]. \quad (\text{A10})$$

Let us now qualitatively describe the effect of anharmonicity of electron oscillations on the damping of beam envelope oscillations. In this analysis we shall assume that the perturbations in electron motion are caused by a fluctuation in the space-charge neutralization factor  $f: f(z) = f_0 + \delta f(z)$ , where  $\delta f(z)$  is a small local perturbation.

Macroscopic parameters of an electron beam (such as a mean radius, radial profile of the beam density, etc.) are determined by the beam microscopic characteristics of individual particles and the beam distribution function. For instance, the mean beam radius  $\bar{r}(z)$  can be determined as

$$\bar{r}(z) = \int r(z, b, \alpha) P(b, \alpha) db d\alpha. \quad (\text{A11})$$

Here  $r(z, b, \alpha)$  is a periodic solution of Eq. (A4) with the amplitude  $b$  and initial phase  $\alpha$  [for instance,  $r = b \cos(kz + \alpha)$ ], and  $P(b, \alpha)$  is the probability function. In a phase-mixed beam,  $P(b, \alpha) = (1/2\pi)P(b)$ , and therefore, the mean radius is constant:  $\bar{r}(z) = \bar{r}_0 = \text{const}$ .

Substituting  $f(z) = f_0 + \delta f(z)$  into Eq. (A4) yields

$$\frac{d^2r}{dz^2} + \frac{2I_b}{I_A \beta^2} (f_0 - \gamma^{-2}) \frac{r}{a^2} - \frac{M^2}{m^2 \gamma^2 r^3 v_z^2} = - \frac{2I_b}{I_A \beta^2} \frac{r}{a^2} \delta f(z). \quad (\text{A12})$$

For the sake of simplicity, assume that the ion perturbation localized near  $z = z_0$  can be described by the  $\delta$  function, and hence, Eq. (A12) can be rewritten as

$$\begin{aligned} \frac{d^2r}{dz^2} + \frac{2I_b}{I_A \beta^2} (f_0 - \gamma^{-2}) \frac{r}{a^2} - \frac{M^2}{m^2 \gamma^2 r^3 v_z^2} \\ = - \frac{2I_b}{I_A \beta^2} \frac{r}{a^2} \Delta f \delta(z - z_0). \end{aligned} \quad (\text{A13})$$

where  $\Delta f$  is the total number of ions in the perturbation.

Consider small oscillations of an electron radius about the equilibrium radius  $r_0$ . For the variable  $x$ , which was determined above by  $r = r_0(1+x)$ , Eq. (A13) reduces to

$$\frac{d^2x}{dz^2} + k^2 x = - \frac{1}{4} k_\beta^2 \frac{\Delta f}{f_0 - \gamma^{-2}} \delta(z - z_0). \quad (\text{A14})$$

Now, in contrast to Eq. (A7), we account for the linear terms only, but the spatial frequency  $k$  depends on the amplitude of electron oscillations  $b$ .

On the left and on the right from the point of perturbation  $z = z_0$ , the solution of Eq. (A14) has the same form,  $x(z) = x_1 \cos[k(b)z + \alpha]$ , however, the amplitudes  $b$  and phases  $\alpha$  are different before and after the perturbation. Their values can be matched by using the boundary conditions at  $z = z_0$ :

$$x|_{z_0-0} = x|_{z_0+0}, \quad \left. \frac{dx}{dz} \right|_{z_0-0} = \left. \frac{dx}{dz} \right|_{z_0+0} - \Delta x'. \quad (\text{A15})$$

Here  $\Delta x'$  is a step in the derivative at this point, which, as follows from Eq. (A14), is equal to

$$\Delta x' = - \frac{1}{4} k_\beta^2 \frac{\Delta f}{f_0 - \gamma^{-2}}. \quad (\text{A16})$$

By using Eq. (A16) and the assumption that the ion perturbation is small, one can readily derive the following expressions for steps in the amplitude and phase:

$$\begin{aligned} \Delta x_1 &\equiv x_1|_{z_0+0} - x_1|_{z_0-0} = - \frac{\sin \phi}{k_\beta} \Delta x', \\ \Delta \alpha &\equiv \alpha|_{z_0+0} - \alpha|_{z_0-0} = - \frac{\cos \phi}{k_\beta x_1} \Delta x'. \end{aligned} \quad (\text{A17})$$

Here  $\phi = kz_0 + \alpha$  is the phase of an unperturbed oscillation at  $z = z_0$ .

Now the solution for  $x$  at  $z \geq z_0$  can be written as

$$x(z) = (x_1 + \Delta x_1) \cos[k(z - z_0) + \phi + \Delta \alpha]. \quad (\text{A18})$$

Substituting Eq. (A18) into Eq. (A11) yields the following expression for the mean value of the beam radius at  $z \geq z_0$ :

$$\bar{r}(z) = r_0 + \frac{1}{2\pi} \int db d\phi P(b) \quad (\text{A19})$$

$$\times \{(b + \Delta b) \cos[k(z - z_0) + \phi + \Delta\alpha]\}$$

$$\approx r_0 + \frac{1}{2\pi} \int db P(b) \int d\phi$$

$$\times \{\Delta b \cos[k(z - z_0) + \phi] - b \Delta\alpha \sin[k(z - z_0) + \phi]\}.$$

Here  $b = r_0 x_1$  is the amplitude of oscillations of a particle radius and  $\Delta b = r_0 \Delta x_1$ . With the use of Eq. (A17), Eq. (A19) can be readily reduced to

$$\bar{r}(z) = r_0 + r_0 \int db P(b) \frac{\Delta x'}{k_\beta} \sin[k(z - z_0)]. \quad (\text{A20})$$

Now, let us take into account that the wave number  $k$  depends on the oscillation amplitude  $b$ :  $k = k_\beta(1 + b^2 R_a)$ , where the anharmonicity parameter  $R_a$  can be easily found from Eq. (A10). Then, Eq. (A20) can be rewritten as

$$\begin{aligned} \bar{r}(z) &= r_0 + r_0 \int db P(b) \frac{\Delta x'}{k_\beta} \sin[k_\beta(1 + R_a b^2)(z - z_0)] \\ &= r_0 + r_0 \left\{ \sin[k_\beta(z - z_0)] \int db P(b) \frac{\Delta x'}{k_\beta} \right. \\ &\quad \times \cos[k_\beta R_a b^2(z - z_0)] + \cos[k_\beta(z - z_0)] \\ &\quad \left. \times \int db P(b) \frac{\Delta x'}{k_\beta} \sin[k_\beta R_a b^2(z - z_0)] \right\}. \quad (\text{A21}) \end{aligned}$$

Equation (A21) shows that at  $z = z_0$  the oscillations of the mean radius of electron oscillations appear. These oscillations have the spatial frequency  $k_\beta$  and they decay with the departure from  $z = z_0$ . A typical distance, which characterizes this damping, can be estimated as

$$l_c \approx \frac{2\pi}{k_{\beta 0} R_a \bar{b}^2}. \quad (\text{A22})$$

Here  $\bar{b}$  is a typical scale of the oscillation amplitude, which depends on the function  $P(b)$ . In our case, the spread in oscillation amplitudes is on the order of the stationary beam envelope radius  $a_*$ ; therefore, accounting for Eq. (A10), the distance  $l_c$  can be estimated as  $l_c \approx 2\pi/k_\beta$ . This estimate shows that the oscillations of the radius decay at the period of betatron oscillations.

- 
- [1] W. H. Bennett, *Phys. Rev.* **45**, 890 (1934).  
[2] J. D. Lawson, *The Physics of Charged-Particle Beams* (Oxford University Press, Oxford, UK, 1977).  
[3] R. B. Miller, *Intense Charged Particle Beams* (Plenum, New York, 1982).  
[4] M. Reiser, *Theory and Design of Charged Particle Beams* (Wiley, New York, 1994).  
[5] G. I. Budker, in *the CERN Symposium on High Energy Accelerators*, edited by N. Rostoker and M. Reiser (CERN, Geneva, Switzerland, 1956), Vol. 1, p. 68.  
[6] R. J. Briggs, J. C. Clark, T. J. Fessenden, R. E. Hester, and E. J. Lauer, in *Proceedings of the 2nd International Topical Conference on High Power Electron and Ion Beam Research and Technology* (Cornell University Press, Ithaca, 1977), Vol. 1, p. 319.  
[7] W. E. Martin, G. J. Caporaso, W. M. Fawley, D. Prosnitz, and A. G. Cole, *Phys. Rev. Lett.* **54**, 685 (1985).  
[8] G. J. Caporaso, F. Rainer, W. E. Martin, D. S. Prono, and A. G. Cole, *Phys. Rev. Lett.* **57**, 1591 (1986).  
[9] H. L. Buchanan, *Phys. Fluids* **30**, 221 (1986).  
[10] R. J. Lipinski, J. R. Smith, I. R. Shokair, K. W. Struve, P. Werner, D. J. Armistead, P. D. Kiekel, I. Molina, and S. Hoggeland, *Phys. Fluids B* **2**, 2764 (1990).  
[11] J. R. Smith, I. R. Shokair, K. W. Struve, E. Schamiloglu, P. W. Werner, and R. J. Lipinski, *IEEE Trans. Plasma Sci.* **19**, 850 (1991).  
[12] R. W. Schumacher, R. Harvey, J. Hyman, and J. Santoru, U.S. Patent No. 4,912,367 (27 March 1990).  
[13] D. M. Goebel, *IEEE Trans. Plasma Sci.* **26**, 263 (1998).  
[14] E. S. Ponti, D. M. Goebel, and R. L. Poeschel, *Proc. SPIE* **2843**, 240 (1996).  
[15] G. S. Nusinovich and Yu. P. Bliokh, *Phys. Rev. E* **62**, 2657 (2000).  
[16] T. Abu-Elfadl, G. S. Nusinovich, A. G. Shkvarunets, Y. Carmel, T. M. Antonsen, Jr., and D. Goebel, *Phys. Rev. E* **63**, 066501 (2001).  
[17] T. Abu-Elfadl, G. S. Nusinovich, A. G. Shkvarunets, Y. Carmel, T. M. Antonsen, Jr., and D. Goebel, *IEEE Trans. Plasma Sci.* (to be published).  
[18] Yu. P. Bliokh and G. S. Nusinovich, *IEEE Trans. Plasma Sci.* **29**, 951 (2001).  
[19] C. C. Cutler, *Proc. IRE* **44**, 61 (1956).  
[20] W. M. Manheimer, H. P. Freund, B. Levush, and T. M. Antonsen, Jr., *Phys. Plasmas* **8**, 297 (2001).  
[21] W. Tighe, D. M. Goebel, and C. B. Thorington, *IEEE Trans. Electron Devices* **48**, 82 (2001).  
[22] E. P. Lee, *Phys. Fluids* **21**, 1327 (1978).  
[23] A. G. Shkvarunets, Y. Carmel, G. S. Nusinovich, T. M. Abu-Elfodl, J. Rodgers, T. M. Antonsen, Jr., V. L. Granatstein, and D. M. Goebel, *Phys. Plasmas*, **9**, 4114 (2002).  
[24] L. D. Landau and E. M. Lifshitz, *Mechanics*, 3rd ed., Course of Theoretical Physics Vol. 1 (Pergamon, Oxford, 1976).